

Band-selective modification of the magnetic fluctuations in Sr_2RuO_4 : A study of substitution effects

Naoki Kikugawa

*School of Physics and Astronomy, University of St. Andrews, St. Andrews, Fife KY16 9SS, United Kingdom;
Venture Business Laboratory, Kyoto University, Kyoto 606-8501, Japan;
and Department of Physics, Kyoto University, Kyoto 606-8502, Japan*

Christoph Bergemann

Cavendish Laboratory, University of Cambridge, Madingley Road, Cambridge CB3 0HE, United Kingdom

Andrew Peter Mackenzie

School of Physics and Astronomy, University of St. Andrews, St. Andrews, Fife KY16 9SS, United Kingdom

Yoshiteru Maeno

*International Innovation Center, Kyoto University, Kyoto 606-8501, Japan
and Department of Physics, Kyoto University, Kyoto 606-8502, Japan*

(Received 19 April 2004; published 29 October 2004)

We report a study of magnetic, thermal, and transport properties of La^{3+} substituted Sr_2RuO_4 , performed in order to investigate the effects of additional electron doping in this correlated metal. A gradual enhancement of the electronic part of specific heat and a more drastic increase of the static magnetic susceptibility were observed in $\text{Sr}_{2-y}\text{La}_y\text{RuO}_4$ with increasing y . Furthermore, the quasi-two-dimensional Fermi-liquid behavior seen in pure Sr_2RuO_4 breaks down near the critical concentration $y_c \sim 0.20$. Combined with a realistic tight-binding model with rigid-band shift of Fermi level, the enhancement of the density of states can be ascribed to the elevation of the Fermi energy toward a van Hove singularity of the thermodynamically dominant γ Fermi-surface sheet. On approaching the van Hove singularity, the effective nesting vector of the γ band shrinks and further enhances the susceptibility near the wave vector $q \sim 0$. We attribute the non-Fermi-liquid behavior to two-dimensional ferromagnetic fluctuations with short range correlations at the van Hove singularity. The observed behavior is in sharp contrast to that of Ti^{4+} substitution in Sr_2RuO_4 which enhances antiferromagnetic fluctuations and subsequently induces incommensurate magnetic ordering associated with the nesting between the other Fermi-surface sheets (α and β). We thus establish that substitution of appropriate chemical dopants can band selectively modify the spin-fluctuation spectrum in the spin-triplet superconductor Sr_2RuO_4 .

DOI: 10.1103/PhysRevB.70.134520

PACS number(s): 74.70.Pq, 74.25.Dw, 74.62.Dh

I. INTRODUCTION

Since the discovery of the superconductivity in the layered perovskite Sr_2RuO_4 ,¹ the material has been the subject of intense research² for the following reasons. First, the superconductivity (with transition temperature $T_c = 1.5$ K) is of unconventional pairing symmetry, most probably spin triplet.² Second, a highly conductive metallic state with mean free path $\ell > 1 \mu\text{m}$ can be achieved, reflecting the well hybridized Ru $4d$ and O $2p$ character of the conduction bands in the stoichiometric material. This made it possible to clarify the detailed electronic structure by means of de Haas–van Alphen experiments^{3–5} and angle-resolved photoemission spectra with⁶ results that are in qualitative agreement with band-structure calculations:^{7,8} the Fermi surface consists of one hole sheet (α) and two electron sheets (β and γ). The α and β bands are formed by the Ru d_{yz} and d_{zx} orbitals, while the γ band has d_{xy} orbital character. On the basis of the cylindrical Fermi-surface topography, normal-state properties are described quantitatively within the framework of a quasi-two-dimensional Fermi liquid.^{5,9}

For a strongly correlated, unconventional superconductor like Sr_2RuO_4 , knowledge of the relationship between the superconductivity and the magnetic fluctuations is of fundamental importance in order to clarify the pairing mechanism. This is strikingly exemplified by a number of f -electron systems and in the high- T_c cuprates, where the superconductivity emerges near regions of magnetic instability.^{10–12} In those cases, the magnetic instability point is reached by driving the magnetic ordering temperature to zero by tuning parameters such as pressure and carrier doping by chemical substitution.¹³ Also, non-Fermi-liquid normal-state behavior is often observed in the vicinity of the quantum critical points.

Spin fluctuations are thought to act as the “magnetic glue” responsible for the superconducting pairing in many of these cases, including, as theoretically suggested, Sr_2RuO_4 .¹⁴ Experimentally, a more direct signature of spin fluctuations can be found in inelastic neutron-scattering measurements. In Sr_2RuO_4 , recent experiments revealed a weak, broadened structure around the wave vector $q \sim 0$, attributed to the excitation from the γ band,¹⁵ in addition to a

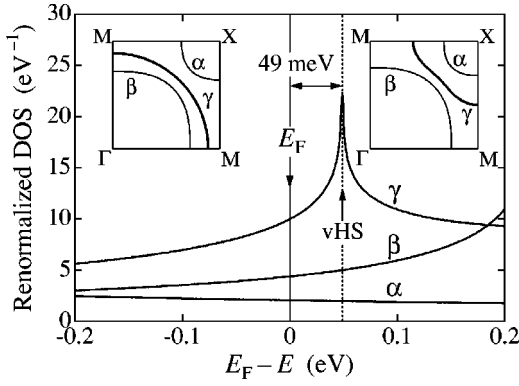


FIG. 1. Partial density of states (DOS) in Sr_2RuO_4 obtained by a tight-binding fit to the experimentally determined Fermi surface (Ref. 5). The Fermi energy is located 49 meV below a van Hove singularity (vHS) of the γ band. Note that the γ Fermi surface changes from an electron pocket (left inset) to a hole pocket (right inset) when the Fermi energy crosses the van Hove singularity at additional electron-doping level of $y_c \sim 0.23/\text{f.u.}$

well-known feature at the incommensurate wave vector $q = Q_{\text{ic}}^{\alpha\beta} \sim (2\pi/3, 2\pi/3, 0)$.¹⁶ The incommensurate wave vector is in accord with a nesting vector between the α and β Fermi surfaces.¹⁷ Attempts have been made to probe the proximity to magnetic quantum critical points by applying strong magnetic field¹⁸ or hydrostatic pressure.¹⁹ These probes have the advantage of being “clean,” i.e., of not introducing disorder, but in the range of parameters used so far on Sr_2RuO_4 , no magnetic instabilities have been discovered.

Although substitution studies involve the introduction of disorder, they have the significant advantage of producing band-specific effects. For example, the substitution of non-magnetic Ti^{4+} ($3d^0$) for Ru^{4+} ($4d^4$) in $\text{Sr}_2\text{Ru}_{1-x}\text{Ti}_x\text{O}_4$ is a powerful probe to enhance *only* the anisotropic antiferromagnetic fluctuations at $Q_{\text{ic}}^{\alpha\beta}$:^{20–22} the ground state in $\text{Sr}_2\text{Ru}_{1-x}\text{Ti}_x\text{O}_4$ changes from spin-triplet superconductivity to incommensurate spin-density-wave (SDW) order²⁰ with the formation of glassy clusters at lower temperatures.^{23,24} Near the onset of magnetic order at $x = x_c \sim 0.025$, breakdown of the Fermi-liquid behavior is observed at low temperatures: the resistivity and specific heat show linear and logarithmic temperature dependence, respectively.²¹ These results indicate that in $\text{Sr}_2\text{Ru}_{1-x}\text{Ti}_x\text{O}_4$ the divergence of spin fluctuations at $Q_{\text{ic}}^{\alpha\beta}$, arising from the nesting between α and β bands, dominates the behavior at x_c .

On the other hand, the role of the magnetic fluctuations of the γ band, which is proposed by some authors to drive the superconductivity in Sr_2RuO_4 ,^{25,26} still remains unclear. The γ band has the largest density of states (DOS) at the Fermi energy and the strongest mass enhancement.⁵ As shown in Fig. 1, in a tight-binding fit to the experimental Fermi-surface geometry, the Fermi energy is located 49 meV below a van Hove singularity (vHS) of the γ band,⁵ corresponding to electron doping of an additional 0.23 electrons per formula unit.^{5,27}

In this paper, we report the effect of nonisovalent cation substitution of Sr^{2+} with La^{3+} , as in $\text{Sr}_{2-y}\text{La}_y\text{RuO}_4$. The primary effect of La doping is the introduction of addi-

tional electrons to the metallic bands at the Fermi energy, because its disorder potential is at its strongest between, rather than within, the RuO_2 planes. La substitution therefore provides a gentle way to study the effect of changing carrier concentration in the correlated metal and unconventional superconductor Sr_2RuO_4 . We achieved electron doping up to $y = 0.27$, where the tight-binding calculation places the Fermi energy of the material well *beyond* the vHS. The main contribution of the enhancement of the DOS is confirmed to be due to the approach towards the vHS of the γ band. At the same time, the nesting wave vector of the γ band is shrinking towards $q \sim 0$ at the vHS, further enhancing the low- q susceptibility. We observe non-Fermi-liquid behavior around the “critical” doping level of $y_c \sim 0.20$ and attribute it to two-dimensional ferromagnetic fluctuations with short-range correlations. The evolution of the ferromagnetic fluctuations with electron doping is in sharp contrast to the enhancement of the antiferromagnetic fluctuations induced by Ti substitution.^{21,22} Throughout this paper, we stress that substitution of appropriate dopants into Sr_2RuO_4 can band selectively modify the magnetic fluctuation spectrum.

II. EXPERIMENT

Single crystals of $\text{Sr}_{2-y}\text{La}_y\text{RuO}_4$ with y up to 0.27 were grown by a floating-zone method in an infrared image furnace (NEC Machinery, model SC-E15HD). Although it was difficult to grow crystals with increasing y because of the necessity of higher temperature and therefore an unstable molten zone during crystal growth, we finally succeeded in obtaining large crystals with typical size of $4 \text{ mm} \times 3 \text{ mm}$ (c axis) $\times 60 \text{ mm}$.

The La concentrations of the crystals were analyzed by electron-probe microanalysis (EPMA). Up to $y = 0.14$, the La substitutes well for Sr. On the other hand, we found that the analyzed La concentration y_a deviates from the nominal La concentration y_n for $y_n > 0.14$: y_a varies roughly as $y_a \sim 0.3y_n + 0.12$. We confirmed tetragonal crystal symmetry for all $\text{Sr}_{2-y}\text{La}_y\text{RuO}_4$ crystals used in this study at room temperature from x-ray measurement. The lattice parameter along the in-plane (a axis) increases by $\sim 0.5\%$ and that perpendicular to the plane (c axis) decreases by $\sim 0.4\%$ continuously with y up to $y = 0.27$. The crystal symmetry and the change of lattice parameter by La doping are consistent with previous work on polycrystals.²⁸

Magnetic susceptibility measurements were performed using a commercial superconducting quantum interference device magnetometer down to 1.8 K (Quantum Design, MPMS-XL). The specific heat C_P was measured by a thermal relaxation method from 0.5 K to 30 K (Quantum Design, model PPMS). The electrical resistivity was measured by standard four-probe dc and ac methods between 4.2 and 300 K and by an ac method between 0.3 and 5 K.

III. RESULTS

A. Static magnetic susceptibility

Figure 2 shows the temperature dependence of the static magnetic susceptibility $\chi(T) = M/H$ of $\text{Sr}_{2-y}\text{La}_y\text{RuO}_4$ with y

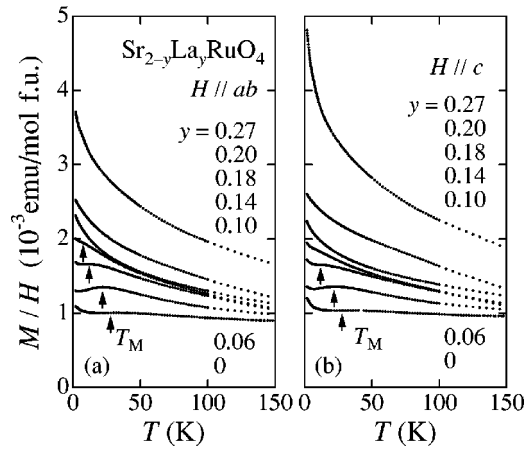


FIG. 2. Temperature dependence of the magnetic susceptibility $\chi(T)=M/H$ of $\text{Sr}_{2-y}\text{La}_y\text{RuO}_4$ with y up to 0.27 in applied field of 1 T along (a) the basal (ab) plane and (b) the c axis. T_M indicates the characteristic temperature at which M/H shows a peak.

up to 0.27 in an applied field of 1 T along the basal (ab) plane (a) and the c axis (b). There is no clear sign of any magnetic ordering for all dopant concentrations in this study.²⁹ It should be noted that the magnetic susceptibility is nearly *isotropic* with respect to the direction of the applied magnetic field. This behavior is in sharp contrast with that of Ti-substituted Sr_2RuO_4 , which exhibits Ising anisotropy.^{23,24} In the normal state of pure Sr_2RuO_4 , $\chi(T)$ shows little temperature dependence (Pauli paramagnetism) with a broad peak around 30 K (denoted as T_M), coinciding with the temperature below which the characteristic signatures of a Fermi liquid are seen. With increasing y , a gradual change to Curie-Weiss-like behavior occurs at high temperature. For $y=0.06$, the behavior with the peak temperature $T_M \sim 22$ K is similar to that seen in the enhanced paramagnet $\text{Sr}_3\text{Ru}_2\text{O}_7$ which possesses a ferromagnetic instability under uniaxial stress.³⁰ T_M shifts to lower temperature with further La doping, and finally for $y > 0.18$ the susceptibility continues to rise sharply

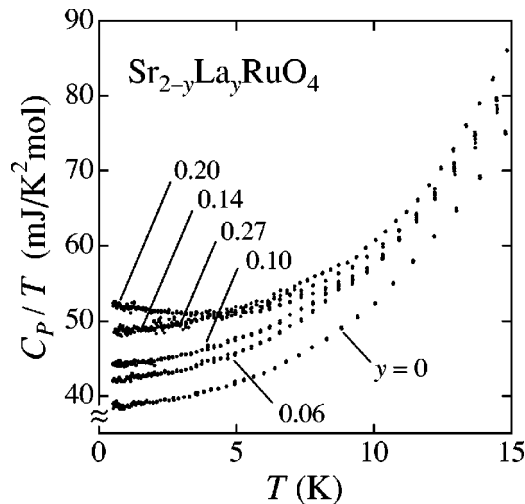


FIG. 3. Temperature dependence of C_p/T in $\text{Sr}_{2-y}\text{La}_y\text{RuO}_4$ up to $y=0.27$. For pure Sr_2RuO_4 ($y=0$) a magnetic field of 0.2 T was applied along the c axis to suppress the superconductivity.

down to the lowest temperatures. The effective magnetic moment p_{eff} , as well as the temperature independent term χ_{Pauli} corresponding to the Pauli paramagnetism, estimated from the Curie-Weiss fitting at higher temperature, increase linearly at the rate of $dp_{\text{eff}}/dy \sim 2\mu_B/\text{La}$ and $d\chi_{\text{Pauli}}/dy \sim 0.7 \times 10^{-3}$ (emu/mol f.u.)/La, respectively.

B. Specific heat

Figure 3 shows the temperature dependence of specific heat divided by temperature C_p/T for $\text{Sr}_{2-y}\text{La}_y\text{RuO}_4$ up to $y=0.27$ and down to $T=0.5$ K. There is no sign of a phase transition, magnetic or otherwise, in line with the susceptibility results. The data for pure Sr_2RuO_4 ($y=0$) were obtained by applying a magnetic field of 0.2 T along the c axis in order to suppress the superconductivity ($T_c=1.44$ K); the data for $\mu_0H=0$ T essentially overlap with the data for 0.2 T for $T > 1.5$ K.³¹ Enhancement of C_p/T with y is clearly observed and is due to the increase of the DOS by electron doping. The enhancement agrees well with the calculations using tight-binding parameters based on the rigid-band

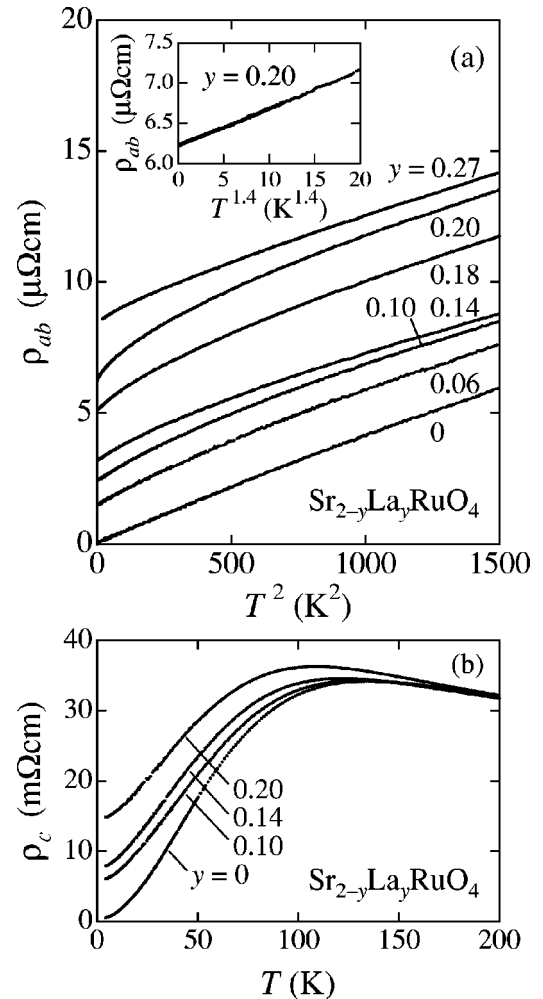


FIG. 4. (a) In-plane resistivity ρ_{ab} plotted against T^2 in $\text{Sr}_{2-y}\text{La}_y\text{RuO}_4$. The inset shows ρ_{ab} vs $T^{1.4}$ with $y=0.20$. (b) Temperature dependence of the c -axis resistivity in $\text{Sr}_{2-y}\text{La}_y\text{RuO}_4$ with several y .

model that each La dopes one free electron.³² Moreover, a clear low-temperature upturn indicating a deviation from simple Fermi-liquid behavior is observed around $y=0.20$. This upturn cannot simply be explained by an impurity effect induced by La doping, because the effect is suppressed for $y=0.27$. This behavior is similar to that seen in Ti-substituted Sr_2RuO_4 in the vicinity of its magnetic ordering.²¹

C. In- and out-of-plane resistivity

Figure 4(a) shows the in-plane resistivity ρ_{ab} for various doping levels y , plotted against T^2 . The residual resistivity ρ_{ab0} , defined by the extrapolation of the low-temperature resistivity to $T=0$ K, increases systematically with y at the rate of $d\rho_{ab0}/dy \sim 40 \mu\Omega \text{ cm}/y$, that is, with a phase shift of impurity scattering $\delta_0 \sim \pi/12$. The enhancement is much smaller than that seen in in-plane substituted Sr_2RuO_4 such as $\text{Sr}_2\text{Ru}_{1-x}\text{Ti}_x\text{O}_4$ and $\text{Sr}_2\text{Ru}_{1-x}\text{Ir}_x\text{O}_4$, where both Ti^{4+} and Ir^{4+} impurities act as unitary potential scatterers with $\delta_0 \sim \pi/2$.³³ This result shows that out-of-plane La^{3+} substitution for Sr^{2+} introduces less severe disorder within the conductive RuO_2 planes.

Another important result in Fig. 4(a) is the breakdown of the Fermi-liquid behavior around $y=0.20$: the T -squared dependence $\rho_{ab}(T) = AT^n + \rho_{ab0}$ with $n=2$, satisfied below about 30 K for pure Sr_2RuO_4 ,⁹ starts to break down with y . This is displayed in Fig. 4(a) by the fact that the temperature range in which the T -squared fitting is valid shrinks with y .³⁴ Also, the coefficient $A \propto m_e^2/n_e$ gradually increases around $y \sim 0.20$, indicating the enhancement of the correlation among electrons by La doping. Here, m_e and n_e are the electron effective mass and carrier density, respectively. Our best fit for $y=0.20$ is obtained with $n=1.4 \pm 0.05$. As added in the inset of Fig. 4, the $T^{1.4}$ behavior is well satisfied between 0.3 and 10 K over more than one decade in temperature. It should be noted that such a deviation from Fermi-liquid behavior is not explained by an effect of disorder by La, because the T -squared behavior is recovered for $y=0.27$ below ~ 7 K.

The temperature dependence of the resistivity along the c axis, ρ_c , for various y is presented in Fig. 4(b). The crossover temperature from nonmetallic behavior ($d\rho_c/dT < 0$) at high temperature to metallic one ($d\rho_c/dT > 0$) at low temperature³⁵ moves monotonically to lower temperature with y as also seen in Ti-substituted Sr_2RuO_4 .²³ The residual resistivity ρ_{c0} increases with doping with a slope $d\rho_{c0}/dy \sim 70 \text{ m}\Omega \text{ cm}/y$. At the same time, the resistivity anisotropy ρ_c/ρ_{ab} at low temperatures remains around 2×10^3 for all dopant concentrations. Also, the temperature region over which a Fermi-liquid-like T^2 law is valid for ρ_c is almost identical to that for ρ_{ab} . This result implies that the quasiparticles can propagate coherently between the RuO_2 layers at low temperatures.

D. Phase diagram of $\text{Sr}_{2-y}\text{La}_y\text{RuO}_4$

The phase diagram of $\text{Sr}_{2-y}\text{La}_y\text{RuO}_4$ is presented in Fig. 5 from (a) the in-plane resistivity and (b) the specific-heat measurements. The substitution of La leads to the suppress-

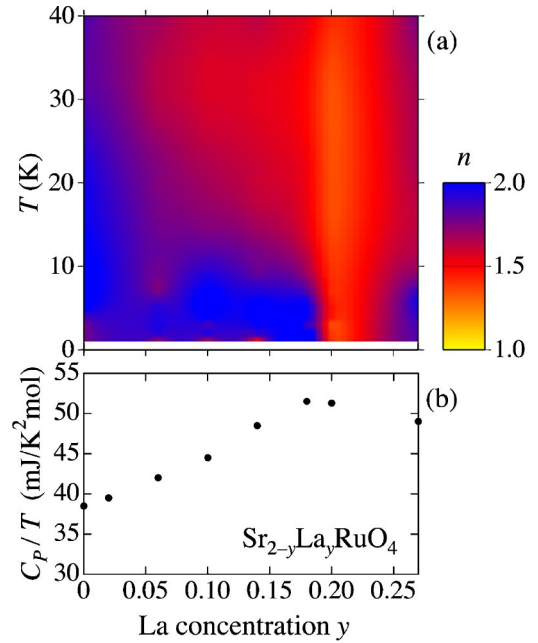


FIG. 5. (a) Temperature and La concentration evolution of the exponent n in $\text{Sr}_{2-y}\text{La}_y\text{RuO}_4$. The exponent n in the nominal expression $\rho_{ab}(T) = \rho_{ab0} + AT^n$ is experimentally derived across the whole phase diagram from the logarithmic derivative $n = d \log(\rho_{ab} - \rho_{ab0}) / d \log T$. For low temperatures, the procedure is quite sensitive to the correct choice of ρ_{ab0} , which we determined self-consistently by asserting that n should be T -independent at the lowest temperatures. (b) The value of C_p/T at 0.5 K as a function of y .

sion of the characteristic temperature of the Fermi-liquid behavior³⁴ in addition to the suppression of T_c around $y \sim 0.03$ as described in Ref. 32. Finally, for $y \sim 0.20$, we can see the breakdown of the Fermi-liquid behavior ($n=1.4$) at low temperature. Also, the enhancement of C_p/T at 0.5 K in Fig. 5(b) suggests deviation from Fermi-liquid behavior in the temperature dependence of C_p/T (Fig. 3). The critical concentration $y \sim 0.20$ is in good agreement with the prediction from tight-binding calculations, where y_c is evaluated as 0.23.^{5,27} This behavior is suggestive of the presence of a quantum critical point near $y \sim 0.20$, but it is not yet conclusive. In particular, no magnetically ordered state has been identified in this study. Further experimental work on this issue is in progress.

IV. DISCUSSION

A. Enhancement of the density of states of the γ band by electron doping in Sr_2RuO_4

Let us first discuss the origin of the enhancement of the density of states by electron doping as seen in the specific heat in Fig. 3. In the band calculation based on a tight-binding model, whose parameters are determined by a fit to the experimentally observed Fermi surfaces,⁵ the Fermi energy is located 49 meV below a vHS of the γ band as shown in Fig. 1, whereas such a singularity is not expected for the α and β bands.^{5,8} The Fermi energy coincides with the singu-

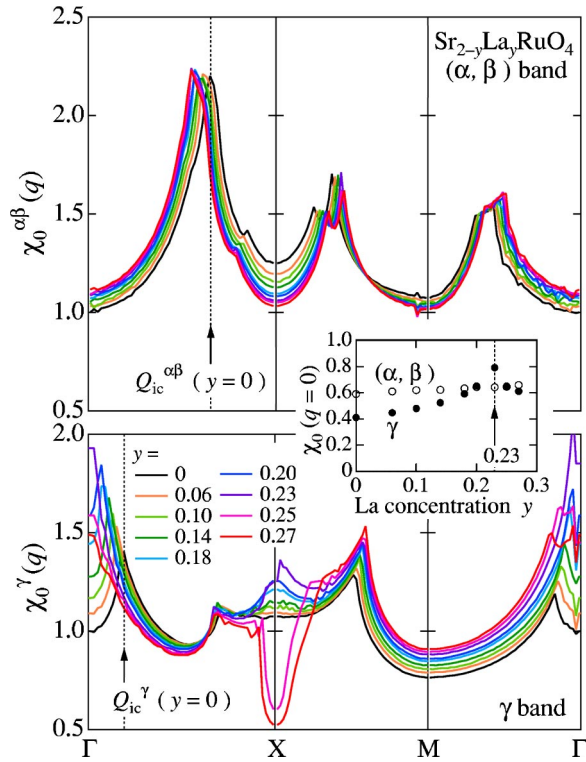


FIG. 6. Momentum dependence of real part of Lindhard susceptibility of $\text{Sr}_{2-y}\text{La}_y\text{RuO}_4$ up to $y=0.27$ based on the realistic tight-binding band structure and a rigid-band shift. The contributions of the α , β bands (upper panel) and the γ band (lower panel) are presented separately, normalized to their values at $q=0$ and $y=0$. The inset shows the La concentration dependence of the static susceptibility ($q=0$) of the α , β bands (open circles) and the γ band (closed circles), with $y=0$ values indicating the relative contributions of (α, β) and γ to the bare density of states.

larity at a doping level of an additional 0.23 electrons/f.u., if a rigid-band model is applicable to this system.⁵ Very recently, we confirmed the rigid-band model to be valid with good quantitative agreement in $\text{Sr}_{2-y}\text{La}_y\text{RuO}_4$ up to $y=0.06$ in a comparison between quantum oscillation measurements (de Haas-van Alphen effect) and tight-binding calculations.³² Here we find experimentally that the critical doping value appears to be 0.20 rather than 0.23 electrons/f.u. (Fig. 5). This indicates a very slight departure from the rigid-band-shift model, possibly because the decrease of the c -axis lattice parameter with La substitution, which lowers the γ band relative to the others, might have non-negligible influence for higher La concentration.³⁶

B. Enhancement of the γ band magnetic susceptibility at $q \sim 0$ by electron doping in Sr_2RuO_4

On the basis of the rigid-band model described above, we now discuss the contributions from the γ band to the magnetic and thermal properties when additional electrons are doped into Sr_2RuO_4 . Figure 6 shows the momentum dependence of the *real* part of the Lindhard susceptibility³⁷ $\chi_0(q)$ expected for $\text{Sr}_{2-y}\text{La}_y\text{RuO}_4$ up to $y=0.27$. Again, the calculation is performed using a tight-binding fit to the experimen-

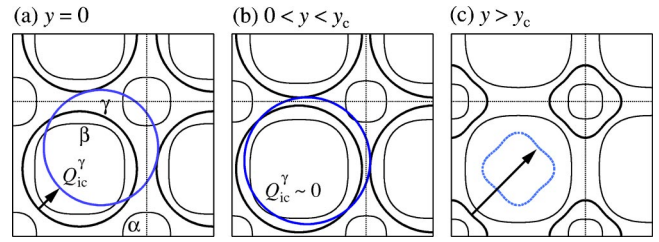


FIG. 7. Sketch of the *weak* Fermi-surface nesting between γ bands for (a) $y=0$, (b) $0 < y < y_c$, and (c) $y > y_c$. Note that the effective nesting-vector Q_{ic}^{γ} shrinks with y . Also, the nesting vector around (π, π) for $y > y_c$ is added in order to explain the suppression of $\chi_0^{\gamma}(q)$ near (π, π) .

tally determined Fermi-surface geometry,⁵ assuming a rigid-band shift. It should be noted that the Lindhard spin susceptibility calculated here is *isotropic* although the electronic structure itself is anisotropic, because the susceptibility formula represents the Zeeman splitting in a metallic state. The figure is separated out into the contributions from the α , β bands (upper panel of Fig. 6) and γ band (lower panel of Fig. 6). The susceptibility is normalized at $q=0$ in pure Sr_2RuO_4 , and the Stoner factor is neglected in this calculation for simplicity. Comparing the contribution from the α/β and γ bands, $\chi_0^{\gamma}(q)$ changes much more dramatically on electron doping than $\chi_0^{\alpha\beta}(q)$ which changes little apart from a small shift in $Q_{ic}^{\alpha\beta}$. This strongly suggests that it is the γ band that mostly affects the change in the magnetic properties by electron doping. Especially, it is clearly found that $\chi_0^{\gamma}(q=0)$ mainly contributes to the enhancement of the total static susceptibility by electron doping, as shown in the inset of Fig. 6.

The peak in $\chi_0^{\gamma}(q)$ at $q = Q_{ic}^{\gamma} \sim (0.2\pi, 0.2\pi)$ as seen in pure Sr_2RuO_4 is explained by weak nesting of the two-dimensional γ bands at the nesting vector Q_{ic}^{γ} , as illustrated in Fig. 7(a). A corresponding structure has only recently been observed in inelastic neutron-scattering measurement,¹⁵ where the experiments detect the *imaginary* part of the dynamical susceptibility.

The main effect of electron doping is that the nesting wave vector Q_{ic}^{γ} shifts to lower q , while both $\chi_0^{\gamma}(q=0)$ and $\chi_0^{\gamma}(Q_{ic}^{\gamma})$ diverge. This divergence of χ_0^{γ} is logarithmic in $(y-y_c)$, but one would expect the Stoner enhancement to lead to a much more dramatic increase in the renormalized susceptibility χ^{γ} . Finally, Q_{ic}^{γ} becomes zero at the van Hove singularity itself, at a critical electron concentration $y_c=0.23$ [Fig. 7(b)]. Beyond the singularity ($y > y_c$), $\chi_0^{\gamma}(q)$ at $q \sim (\pi, \pi)$ (the X point) is dramatically suppressed, as seen for $y=0.25$ and 0.27 in Fig. 6(b). Here the Fermi energy is higher than the vHS, and as illustrated in the right inset of Fig. 1, the Fermi surface of the γ band changes from an electron pocket to a hole one. As seen in Fig. 7(c), the wave vector (π, π) then fails to connect the γ sheet with itself, leading to a substantial loss of susceptibility near the X point.

Using the above Lindhard calculation, although the Stoner factor is neglected in this calculation, we can qualitatively explain most of the evolution of the results of our static susceptibility ($q=0$) with La doping (Fig. 2). The marked increase of the observed susceptibility with La doping is ex-

plained in terms of the enhanced density of states at the Fermi level as the vHS is approached and Q_{ic}^{γ} shrinks to zero. We note again that the Lindhard susceptibility is always *isotropic*, in accordance with our experiment (Fig. 2), since it essentially represents the Zeeman splitting in the metallic state. This holds despite the quasi-two-dimensionality of the electronic structure and spin-fluctuation spectrum. However, we note that there must also be another contribution to the susceptibility as well, because it is not easy to account in the above analysis either for the strength of the temperature dependence for $y > 0.1$ or for the behavior seen in at $y = 0.27$, for which an overall decrease of χ is predicted.

C. Evolution of ferromagnetic fluctuations and their relation to the non-Fermi-liquid behavior

We now focus on the non-Fermi-liquid behavior around $y \sim 0.20$, where we observe a low-temperature upturn in the specific heat and a clear deviation from T^2 behavior in the resistivity. We have described in the preceding section that we expect a strong enhancement of ferromagnetic fluctuations when the Fermi level crosses the vHS—evaluated at $y_c = 0.23$ in the rigid-band-shift model⁵—due to the enhanced DOS arising from the shift of the two-dimensional nesting-vector Q_{ic}^{γ} toward $q = 0$. The enhanced DOS is also expected to affect the specific-heat coefficient C_p/T .

The observed non-Fermi-liquid resistivity exponent of $n = 1.4$ for $y = 0.20$, as shown in the inset of Fig. 4(a), is in good agreement with the expectation of the self-consistent renormalization theory with $n = 4/3$ for two-dimensional ferromagnetic spin fluctuations.³⁸ The essential ingredient here is the two-dimensional nesting-vector $Q_{ic}^{\gamma} = 0$. The situation is quite different in the Ti-substituted system $Sr_2Ru_{1-x}Ti_xO_4$, where at $x_c = 0.025$ the non-Fermi-liquid behavior is observed as well, but in that case with a *linear* ($n = 1$) resistivity power law.²¹ The origin of this behavior lies in the diverging *antiferromagnetic* fluctuations originating from the finite (incommensurate) nesting-vector $Q_{ic}^{\alpha\beta}$ between the α and β sheets.³⁹

Finally, let us discuss the absence of magnetic ordering in $Sr_{2-y}La_yRuO_4$ around $y = y_c$ in our current study. Deviations from Fermi-liquid behavior are often observed around a quantum critical point in the vicinity of magnetic order.¹³ Indeed, the expected divergence of the Lindhard susceptibility would strongly promote (ferro)magnetic ordering. In $Sr_{2-y}La_yRuO_4$ up to $y = 0.27$, however, we have seen no clear evidence for emergence of magnetic ordering, although the non-Fermi-liquid behavior is clearly observed around $y \sim 0.20$, indicating the immediate vicinity of the vHS. One possibility for the absence of the magnetic ordering seems to be that the magnetic correlation length is short as seen in the inelastic neutron scattering in pure Sr_2RuO_4 ;¹⁵ the magnetic excitations originating from the γ band are widely spread

around $q \sim 0$. The short-range correlation reminds us of the case of the $Sr_2Ru_{1-x}Ti_xO_4$ with $x = 0.09$. Elastic neutron-scattering measurements on this system revealed a clear SDW ordering below 25 K with the nesting-vector $Q_{ic}^{\alpha\beta}$. However, the correlation length at the ordered state is as short as ~ 5 nm (Ref. 20) and no anomaly corresponding to the transition is observed in the specific heat.²¹ The correlation length in $Sr_{2-y}La_yRuO_4$ has not been measured yet, although it will be important to do so, in order to detect the evolution of the spin fluctuations at $q \sim 0$ by La doping.

V. SUMMARY

By minimizing the disorder level by substituting La^{3+} for Sr^{2+} , we reported the effect of additional electron doping in Sr_2RuO_4 . The enhancement of the DOS by additional electrons is well explained by a rigid-band model based on the realistic tight-binding calculation. The result can be mainly ascribed to the approach of the Fermi energy towards a vHS of γ band, which is positioned at a doping level $y_c \sim 0.20$, 49 meV above the Fermi level in pristine Sr_2RuO_4 . The enhancement of the magnetic susceptibility by electron doping toward the vHS can be viewed in terms of the shrinking of the nesting vector of the γ band from $Q_{ic}^{\gamma} \sim (0.2\pi, 0.2\pi, 0)$ at $y = 0$ to $Q_{ic}^{\gamma} \sim 0$ at $y \sim y_c$ on the basis of a calculation of the Lindhard susceptibility. The non-Fermi-liquid behavior around $y = 0.20$ is explained in terms of the two-dimensional ferromagnetic spin fluctuations with short-range correlation. On the other hand, Ti substitution induces magnetic ordering associated with the nesting between other α and β Fermi-surface sheets, so appropriate dopants can selectively enhance the spin fluctuations of different bands in Sr_2RuO_4 . Thus, we stress that the layered ruthenate Sr_2RuO_4 is a prototype multiband metal in which we can understand the physical properties with a surprising level of precision, given the correlated nature of the electronic state in this material.

ACKNOWLEDGMENTS

The authors thank K. M. Shen, M. Braden, S. R. Julian, T. Nomura, Kosaku Yamada, and R. Werner for useful discussions. They also thank H. Fukazawa and H. Yaguchi for technical support and discussions, M. Yoshioka for technical support, Y. Shibata, J. Hori, Takashi Suzuki, and Toshizo Fujita for EPMA measurements at Hiroshima University. This work was supported by the Grant-in-Aid for Scientific Research (S) from the Japan Society for Promotion of Science (JSPS), by the Grant-in-Aid for Scientific Research on Priority Area “Novel Quantum Phenomena in Transition Metal Oxides” from the Ministry of Education, Culture, Sports, Science and Technology. One of the authors (N.K.) is supported by JSPS Postdoctoral Fellowships for Research Abroad.

- ¹Y. Maeno, H. Hashimoto, K. Yoshida, S. Nishizaki, T. Fujita, J. G. Bednorz, and F. Lichtenberg, *Nature (London)* **372**, 532 (1994).
- ²A. P. Mackenzie and Y. Maeno, *Rev. Mod. Phys.* **75**, 657 (2003).
- ³A. P. Mackenzie, S. R. Julian, A. J. Diver, G. J. McMullan, M. P. Ray, G. G. Lonzarich, Y. Maeno, S. Nishizaki, and T. Fujita, *Phys. Rev. Lett.* **76**, 3786 (1996).
- ⁴C. Bergemann, S. R. Julian, A. P. Mackenzie, S. NishiZaki, and Y. Maeno, *Phys. Rev. Lett.* **84**, 2662 (2000).
- ⁵C. Bergemann, A. P. Mackenzie, S. R. Julian, D. Forsythe, and E. Ohmichi, *Adv. Phys.* **52**, 639 (2003).
- ⁶A. Damascelli, D. H. Lu, K. M. Shen, N. P. Armitage, F. Ronning, D. L. Feng, C. Kim, Z.-X. Shen, T. Kimura, Y. Tokura, Z. Q. Mao, and Y. Maeno, *Phys. Rev. Lett.* **85**, 5194 (2000).
- ⁷T. Oguchi, *Phys. Rev. B* **51**, 1385 (1995).
- ⁸D. J. Singh, *Phys. Rev. B* **52**, 1358 (1995).
- ⁹Y. Maeno, K. Yoshida, H. Hashimoto, S. Nishizaki, S. Ikeda, M. Nohara, T. Fujita, A. P. Mackenzie, N. E. Hussey, J. G. Bednorz, and F. Lichtenberg, *J. Phys. Soc. Jpn.* **66**, 1405 (1997).
- ¹⁰N. D. Mathur, F. M. Grosche, S. R. Julian, I. R. Walker, D. M. Freye, R. K. W. Haselwimmer, and G. G. Lonzarich, *Nature (London)* **394**, 39 (1998).
- ¹¹S. S. Saxena, P. Agarwal, K. Ahilan, F. M. Groche, R. K. W. Haselwimmer, M. J. Steiner, E. Pugh, I. R. Walker, S. R. Julian, P. Monthoux, G. G. Lonzarich, A. Huxley, I. Sheikin, D. Braithwaite, and J. Flouquet, *Nature (London)* **406**, 587 (2000).
- ¹²G. Aeppli, T. E. Mason, S. M. Hayden, H. A. Mook, and J. Kulda, *Science* **278**, 1432 (1997).
- ¹³G. R. Stewart, *Rev. Mod. Phys.* **73**, 797 (2001).
- ¹⁴P. Monthoux and G. G. Lonzarich, *Phys. Rev. B* **59**, 14 598 (1999).
- ¹⁵M. Braden, Y. Sidis, P. Bourges, P. Pfeuty, J. Kulda, Z. Mao, and Y. Maeno, *Phys. Rev. B* **66**, 064522 (2002).
- ¹⁶Y. Sidis, M. Braden, P. Bourges, B. Hennion, S. NishiZaki, Y. Maeno, and Y. Mori, *Phys. Rev. Lett.* **83**, 3320 (1999).
- ¹⁷I. I. Mazin and D. J. Singh, *Phys. Rev. Lett.* **82**, 4324 (1999).
- ¹⁸C. Bergemann, S. R. Julian, A. P. Mackenzie, A. W. Tyler, D. E. Farrell, Y. Maeno, and S. NishiZaki, *Physica C* **317–318**, 444 (1999).
- ¹⁹D. Forsythe, S. R. Julian, C. Bergemann, E. Pugh, M. J. Steiner, P. L. Alireza, G. J. McMullan, F. Nakamura, R. K. W. Haselwimmer, I. R. Walker, S. S. Saxena, G. G. Lonzarich, A. P. Mackenzie, Z. Q. Mao, and Y. Maeno, *Phys. Rev. Lett.* **89**, 166402 (2002).
- ²⁰M. Braden, O. Friedt, Y. Sidis, P. Bourges, M. Minakata, and Y. Maeno, *Phys. Rev. Lett.* **88**, 197002 (2002).
- ²¹N. Kikugawa and Y. Maeno, *Phys. Rev. Lett.* **89**, 117001 (2002).
- ²²K. Ishida, Y. Minami, Y. Kitaoka, S. Nakatsuji, N. Kikugawa, and Y. Maeno, *Phys. Rev. B* **67**, 214412 (2003).
- ²³M. Minakata and Y. Maeno, *Phys. Rev. B* **63**, 180504(R) (2001).
- ²⁴K. Pucher, J. Hemberger, F. Mayr, V. Fritsch, A. Loidl, E.-W. Scheidt, S. Klimm, R. Horny, S. Horn, S. G. Ebbinghaus, A. Reller, and R. J. Cava, *Phys. Rev. B* **65**, 104523 (2002).
- ²⁵M. Sigrist, D. Agterberg, A. Furusaki, C. Honerkamp, K. K. Ng, T. M. Rice, and M. E. Zhitomirsky, *Physica C* **317–318**, 134 (1999).
- ²⁶T. Nomura and K. Yamada, *J. Phys. Soc. Jpn.* **69**, 3678 (2000); **71**, 1993 (2002).
- ²⁷In Ref. 8, the additional electrons that Fermi energy approaches the singularity is evaluated as 0.2 electrons/f.u.
- ²⁸H. Hashimoto, Master thesis, Hiroshima University.
- ²⁹Tiny hystereses between zero-field-cooled and field-cooled processes are observed at low temperature. We concluded that this is not due to an intrinsic behavior, but probably due to inclusion of ferromagnet SrRuO₃ (or Sr_{1-y}La_yRuO₃) with an estimated amount of less than ~100 ppm, low enough to be invisible in the x-ray measurements. The ferromagnetism in Sr_{1-y}La_yRuO₃ is gradually suppressed with La concentration (Ref. 40).
- ³⁰S. Ikeda, Y. Maeno, S. Nakatsuji, M. Kosaka, and Y. Uwatoko, *Phys. Rev. B* **62**, R6089 (2000); S. Ikeda, N. Shirakawa, T. Yanagisawa, Y. Yoshida, S. Koikegami, S. Koike, M. Kosaka, and Y. Uwatoko, *J. Phys. Soc. Jpn.* **73**, 1322 (2004).
- ³¹A. P. Mackenzie, S. Ikeda, Y. Maeno, T. Fujita, S. R. Julian, and G. G. Lonzarich, *J. Phys. Soc. Jpn.* **67**, 385 (1998).
- ³²N. Kikugawa, A. P. Mackenzie, C. Bergemann, R. A. Borzi, S. A. Grigera, and Y. Maeno, *Phys. Rev. B* **70**, 060508(R) (2004).
- ³³N. Kikugawa, A. P. Mackenzie, and Y. Maeno, *J. Phys. Soc. Jpn.* **72**, 237 (2003).
- ³⁴As seen in Fig. 5(a), a deviation from the T -squared behavior around $y \sim 0.05$ is observed. This might suggest a connection with fluctuations near the critical disorder for the disappearance of superconductivity [$y \sim 0.03$ in Sr_{2-y}La_yRuO₄ (Ref. 32)] as theoretically proposed (Ref. 41), although the predicted temperature dependence of the fluctuation conductivity is very weak.
- ³⁵K. Yoshida, Y. Maeno, S. Nishizaki, S. Ikeda, and T. Fujita, *J. Low Temp. Phys.* **105**, 1593 (1996).
- ³⁶K. M. Shen (private communication).
- ³⁷For instance, K. Yoshida, *Theory of Magnetism* (Springer-Verlag, Berlin, 1996).
- ³⁸M. Hatatani and T. Moriya, *J. Phys. Soc. Jpn.* **64**, 3434 (1995).
- ³⁹We note that our analysis of ρ_{ab} may be simplistic, since resistive exponents in other ruthenates are sensitive to disorder, as reported in Ref. 42.
- ⁴⁰H. Nakatsugawa, E. Iguchi, and Y. Oohara, *J. Phys.: Condens. Matter* **14**, 415 (2002).
- ⁴¹H. Adachi and R. Ikeda, *J. Phys. Soc. Jpn.* **70**, 2848 (2001).
- ⁴²L. Capogna, A. P. Mackenzie, R. S. Perry, S. A. Grigera, L. M. Galvin, P. Raychaudhuri, A. J. Schofield, C. S. Alexander, G. Cao, S. R. Julian, and Y. Maeno, *Phys. Rev. Lett.* **88**, 076602 (2002), and references therein.